ELSEVIER

1 May 1996

OPTICS COMMUNICATIONS

Optics Communications 126 (1996) 167–174

*Full length article*

# Modulational instability of quasi-plane-wave optical beams biased in photorefractive crystals

M.I. Carvalho, S.R. Singh, D.N. Christodoulides

*Department of Electrical Engineering and Computer Science, Lehigh University, Bethlehem, PA 18015, USA*

Received 17 October 1995; accepted 28 November 1995

**Abstract**

The modulational instability of quasi-plane-wave optical beams in biased photorefractive media is investigated under steady-state conditions. The spatial growth rate of the sideband perturbations is obtained by globally treating the space-charge field. Our analysis indicates that the growth rates depend on the strength of the externally applied electric field and, moreover, on the ratio of the optical beam's intensity to that of the dark irradiance. Our results are then compared to previous local treatments of the space-charge field equation. The two approaches are found to be in good agreement in the low spatial-frequency regime provided that the external bias field is sufficiently high. Conversely, in the high spatial-frequency region notable differences may exist. Relevant examples are provided.

## 1. Introduction

In a recent experimental study [1], optical spatial screening solitons have been observed for the first time in strontium barium niobate (SBN). Soliton states of this sort are known to occur when the process of diffraction is exactly balanced by light-induced photorefractive (PR) waveguiding [2]. This latter process is possible provided that the PR crystal is externally biased [3,4]. Unlike their quasi-steady-state counterparts [5–7], which are short-lived entities, screening solitons exist under steady-state conditions. As previous theoretical studies have shown [3,4], the spatial width and shape of these self-trapped states are entirely determined by two parameters, namely the magnitude of the externally applied electric field and the ratio of their peak intensity to that of the dark irradiance. Of course, at this point, it would be of interest to know if such PR systems can also exhibit modulational instability (MI) [8]. In a rather loose context, MI can be considered as a precursor of soliton formation, and its existence is often tied to that of optical solitons. In the spatial domain, MI manifests itself as filamentation of a broad optical beam through the spontaneous growth of spatial-frequency sidebands. It is interesting to note that, in the spatio–temporal regime, induced MI has been successfully demonstrated by externally controlling the repetition rate of a short pulse train [9]. Very recently, Castillo et al. [10] have provided experimental evidence of such induced MI in a PR bismuth titanium oxide ($Bi_{12}TiO_{20}$ or BTO) crystal, which can be considered as the spatial analog of Ref. [9]. Moreover, in this latter study [10], the MI gain was analytically obtained by considering only local effects in the space-charge field. Nevertheless, at this point, it is not very clear to what extent such a local treatment can accurately describe the MI process.

In this Communication we investigate the modulational instability of broad (quasi-plane-wave) optical


*SSDI* 0030-4018(95)00743-1

beams in biased PR media under steady-state conditions. The spatial growth rate of the sideband perturbations is obtained by globally treating the space-charge field equation. Our analysis indicates that the MI growth rate depends on the strength and polarity of the externally applied electric field and, moreover, on the ratio of the optical beam's intensity to that of the dark irradiance. Our results are then compared to previous local treatments of the space-charge field [10]. The two approaches are found to be in good agreement in the low spatial-frequency regime provided that the external bias field is sufficiently high. In this region, our results show that the instability growth rate increases with the bias field and that it attains a maximum when the optical beam intensity is approximately equal to the dark irradiance. Conversely, in the high spatial-frequency regime, notable differences may exist between these two approaches. Pertinent examples are provided.

## 2. Problem formulation

To study the modulational instability of a quasi-plane-wave (broad) optical beam in a biased PR crystal, let us first consider an optical wave that propagates along the $z$-axis and is allowed to diffract only along the $x$-direction. In doing so, our diffraction theory is one-dimensional and any $y$-dependent perturbations have been implicitly omitted [11]. For demonstration purposes, let the PR crystal be SBN, with its optical $c$-axis oriented along the $x$-direction. Moreover, let us assume that the optical beam is linearly polarized along $x$ and that the external bias electric field is applied in the same direction. Under these conditions, the perturbed extraordinary refractive index $n_e'$ (along the $c$-axis) is given by [12] $(n_e')^2 = n_e^2 - n_e^4 r_{33} E_{sc}$ where $r_{33}$ is the electro-optic coefficient involved, $n_e$ is the unperturbed extraordinary index of refraction and $\boldsymbol{E}_{sc} = E_{sc}\hat{\boldsymbol{x}}$ is the space-charge field in this PR sample. In this case, by employing standard procedures, we readily obtain the following paraxial equation of diffraction [4]

$$i\frac{\partial U}{\partial z} + \frac{1}{2k}\frac{\partial^2 U}{\partial x^2} - \frac{k_0}{2}\left(n_e^3 r_{33} E_{sc}\right)U = 0, \qquad (1)$$

where the optical field $\mathscr{E}$ has been expressed in terms of a dimensionless slowly-varying envelope $U$, that is, $\mathscr{E} = \hat{\boldsymbol{x}}(2\eta_0 I_d/n_e)^{1/2} U(x, z)\exp(ikz)$. The beam power density has been scaled with respect to the dark irradiance $I_d$ [13], i.e. $I(x, z) = |U|^2 I_d$, and the wavevector $k$ is given by $k = k_0 n_e = (2\pi/\lambda_0)n_e$, where $\lambda_0$ is the free-space wavelength of the lightwave employed. For simplicity, any loss effects have been neglected in deriving Eq. (1).

The space-charge field $E_{sc}$ can then be obtained from the transport model of Kukhtarev et al. [14]. Under steady-state conditions and for typical PR media, the space-charge field $E_{sc}$ is known to obey the following differential equation [4]

$$E_{sc} = E_0 \frac{1}{\left[1 + |U|^2\right]}\left(1 + \frac{\epsilon_0\epsilon_r}{eN_A}\frac{\partial E_{sc}}{\partial x}\right) - \frac{K_B T}{e}\frac{\left[\partial(|U|^2)/\partial x\right]}{\left[1 + |U|^2\right]} + \frac{K_B T}{e}\frac{\epsilon_0\epsilon_r}{eN_A}\left(1 + \frac{\epsilon_0\epsilon_r}{eN_A}\frac{\partial E_{sc}}{\partial x}\right)^{-1}\frac{\partial^2 E_{sc}}{\partial x^2}, \qquad (2)$$

where $U(x, z)$ is assumed to be a bright-like beam, i.e. $|U|^2 = 0$ at $x \to \pm\infty$, and $E_0$ represents the value of the space-charge field in the dark regions of the PR crystal. In Eq. (2), $K_B$ is Boltzmann's constant, $T$ is the absolute temperature, $e$ is the electron charge, $N_A$ represents the acceptor or trap density, and $\epsilon_r$ is the static relative permittivity.

For broad or quasi-plane-wave planar beams, the optical beam envelope $U$ remains relatively constant over a large range of $x$. As a result, the diffraction term in Eq. (1) $((2k)^{-1}(\partial^2 U/\partial x^2))$ as well as the spatial derivatives of $E_{sc}$ and $|U|^2$ in Eq. (2) can be omitted. Therefore, in this region, the space-charge field can be evaluated and it is approximately given by $E_{sc} = E_0/(1 + |U|^2)$. In turn, Eq. (1) can be readily solved and its broad beam solution is given by

$$U = r^{1/2}\exp\{-i\beta[E_0/(1+r)]z\}, \qquad (3)$$

where the parameter $\beta$ is defined as $\beta = [(k_0 n_e^3 r_{33})/2]$ and the quantity $r$ stands for the ratio of the optical beam intensity to that of the dark irradiance. The stability of this solution is then investigated by adding a spatial perturbation $\epsilon(x, z)$ to the stationary result of Eq. (3) in the following way:

$$U = \left[r^{1/2} + \epsilon(x, z)\right]\exp\{-i\beta[E_0/(1+r)]z\}, \qquad (4)$$

where the magnitude of the complex perturbation $\epsilon$ is assumed to be as usual [15] much smaller than the amplitude of the quasi-plane-wave solution, i.e. $|\epsilon| \ll r^{1/2}$.

In the next section we will investigate the possible growth of this weak perturbation by globally treating the space-charge field equation, Eq. (2).

## 3. Global treatment of modulational instability

In this section the MI process is investigated in a global fashion by implicitly taking into account all higher-order effects in the space-charge field equation, Eq. (2). We begin our analysis by substituting the perturbed envelope $U$, given by Eq. (4), in Eqs. (1) and (2). By linearizing in $\epsilon$, the following coupled set of equations is obtained:

$$\mathrm{i}\frac{\partial \epsilon}{\partial z} + \frac{1}{2k}\frac{\partial^2 \epsilon}{\partial x^2} - \beta E(r^{1/2} + \epsilon) = 0 \tag{5}$$

and

$$E - \gamma\frac{\partial E}{\partial x} - \Delta\frac{\partial^2 E}{\partial x^2} = -\frac{r^{1/2}}{(1+r)}\left[E_{01}(\epsilon + \epsilon^*) + \frac{K_B T}{e}\left(\frac{\partial \epsilon}{\partial x} + \frac{\partial \epsilon^*}{\partial x}\right)\right], \tag{6}$$

where we have defined $E = E_{SC} - E_0/(1+r)$, $E_{01} = E_0/(1+r)$, $\gamma = E_{01}[\epsilon_0 \epsilon_r/(eN_A)]$ and $\Delta = (K_B T/e)[\epsilon_0 \epsilon_r/(eN_A)]$. Eq. (6) can then be treated by means of a Fourier transform. In doing so, the space-charge field, $\hat{E}$, in the spatial-frequency domain, $k_x$ is given by

$$\hat{E} = -\frac{r^{1/2}}{(1+r)}\left\{\frac{E_{01} + \mathrm{i}[\gamma E_{01} k_x + k_x (K_B T/e)(1 + \Delta k_x^2)]}{(1 + \Delta k_x^2)^2 + k_x^2 \gamma^2}\right\} \times (\hat{\epsilon} + \hat{\epsilon}^*), \tag{7}$$

where $\hat{\epsilon}$ is the Fourier transform of the spatial perturbation in the $k_x$-space. If we now assume that the spatial perturbation $\epsilon(x, z)$ is composed of two sideband plane-waves, i.e.

$$\epsilon = a(z)\exp(\mathrm{i}px) + b(z)\exp(-\mathrm{i}px), \tag{8}$$

we then easily find that $(\hat{\epsilon} + \hat{\epsilon}^*) = 2\pi[(a + b^*)\delta(k_x - p) + (b + a^*)\delta(k_x + p)]$, where $\delta(k_x)$ is a delta function. By substituting this latter form of $(\hat{\epsilon} + \hat{\epsilon}^*)$ back into Eq. (7) and by taking an inverse Fourier transform, we obtain the space-charge field in real space, that is

$$E = -\frac{1}{\beta r^{1/2}}[G(p)(a + b^*)\exp(\mathrm{i}px) + G^*(p)(a^* + b)\exp(-\mathrm{i}px)], \tag{9}$$

where the function $G(p)$ has been defined as follows

$$G(p) = \beta\frac{r}{(1+r)} \times\left\{\frac{E_{01} + \mathrm{i}[(\gamma E_{01} + K_B T/e)p + \Delta(K_B T/e)p^3]}{(1 + \Delta p^2)^2 + \gamma^2 p^2}\right\}. \tag{10}$$

By substituting Eqs. (8) and (9) into Eq. (5) and by keeping only synchronous terms leads to the following coupled differential equations:

$$\mathrm{i}\frac{\mathrm{d}a}{\mathrm{d}z} - \frac{p^2}{2k}a + G(p)(a + b^*) = 0, \tag{11a}$$

$$\mathrm{i}\frac{\mathrm{d}b}{\mathrm{d}z} - \frac{p^2}{2k}b + G^*(p)(a^* + b) = 0. \tag{11b}$$

Eqs. (11a) and (11b) can then be readily decoupled into an equivalent set of ordinary differential equations:

$$\frac{\mathrm{d}^2 a}{\mathrm{d}z^2} = \left[\frac{p^2}{k}G(p) - \frac{p^4}{4k^2}\right]a, \tag{12a}$$

$$\frac{\mathrm{d}^2 b}{\mathrm{d}z^2} = \left[\frac{p^2}{k}G^*(p) - \frac{p^4}{4k^2}\right]b. \tag{12b}$$

From this set, the global instability gain, $g_{gl}$, can be directly obtained and it is given by

$$g_{gl} = \mathrm{Re}\left\{\left(\frac{p^2}{k}G(p) - \frac{p^4}{4k^2}\right)^{1/2}\right\}, \tag{13}$$

where Re{ } represents the real part of a complex variable. A close inspection of Eq. (13) reveals that the MI gain is an even function of $p$ and that it is zero at the origin, i.e. at $p = 0$.

We will now illustrate these results by means of relevant examples. The SBN crystal parameters are here taken to be $n_e = 2.33$, $r_{33} = 237$ pm/V, $\epsilon_r = 880$ and $N_A = 3.7 \times 10^{22}$ m$^{-3}$ [16]. The PR crystal

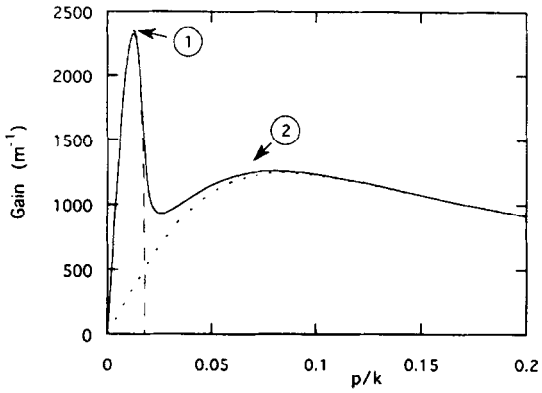


Fig. 1. Global MI gain (solid line), local MI gain (long-dashed line) as well as TWM gain (short-dashed line) as a function of $p/k$ when $E_0 = 5 \times 10^5$ V/m and $r = 1$.

is assumed to be at room temperature and, moreover, let $\lambda_0 = 0.5$ μm. For this set of values, $\beta$ and $k$ are found to be $\beta = 1.88 \times 10^{-2}$ $V^{-1}$ and $k = 2.93 \times 10^7$ $m^{-1}$. Fig. 1 depicts the MI gain given by Eq. (13) (solid line curve) as a function of the dimensioneless quantity $p/k$ when $E_0 = 5 \times 10^5$ V/m and $r = 1$. Since the MI gain is symmetric with respect to $p$, only the positive $p$-branch is plotted. Moreover, it is important to note that the dimensioneless ratio $p/k$ represents the angle (in radians) at which the plane-wave components of the $\epsilon(x, z)$ perturbation propagate with respect to the quasi-plane-wave optical beam. Fig. 1 shows that, in this case, the MI gain curve attains two different peaks, one in the low spatial-frequency domain, denoted as peak 1, and another one, peak 2, in the high spatial-frequency region. The two spatial-frequencies at which these two peaks occur, $p_{p1}$ and $p_{p2}$, as well as the corresponding values of the MI gain, i.e. $g_{p1}$ and $g_{p2}$, are found to depend on both the external bias field, $E_0$, and the ratio of the optical beam intensity to that of the dark irradiance, $r$. In general, the effect of $E_0$ and $r$ on the overall MI gain curve can always be obtained from Eq. (13). Nevertheless, this dependence is somewhat involved and, thus, it can only be investigated by considering each one of them in isolation. Let us first begin by considering the effects arising from the bias field $E_0$. Figs. 2a and 2b illustrate the dependence of the two peak spatial-frequencies and their respective MI gains on $E_0$ when $r = 1$. A careful examination of these figures reveals that peak 1 exists only for positive polarities of the external bias field. Moreover, Figs. 2a and 2b show that both $p_{p1}$ and $g_{p1}$ increase with the magnitude of $E_0$. Conversely, $p_{p2}$ and $g_{p2}$ are found to be symmetric with respect to the polarity of $E_0$, which means that they only depend on its absolute strength. Furthermore, Fig. 2b shows that $g_{p2}$ also increases with the absolute strength of the bias field. It is also apparent from Fig. 2b that, after a particular value of $E_0$, $g_{p1}$ exceeds $g_{p2}$, which in turn implies that the MI gain arising from peak 1 (in the low spatial-frequency region) will dominate the process. On the other hand, Figs. 3a and 3b depict the variation of the two gain peaks as a function of $r$, when $E_0 = 5 \times 10^5$ V/m. As one can see, the spatial-frequency as well as the gain corresponding to peak 1 attain a maximum when $r \cong 1$ and, moreover, $g_{p1}$ tends to quickly decrease when $r \ll 0.1$ and $r \gg 10$.

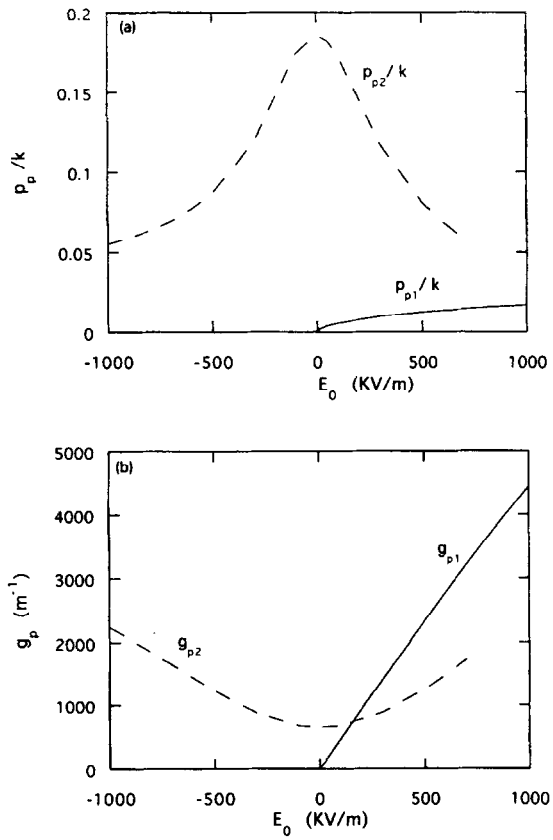


Fig. 2. Dependence of (a) the two global peak spatial-frequencies and (b) of their respective gains on $E_0$ when $r = 1$.

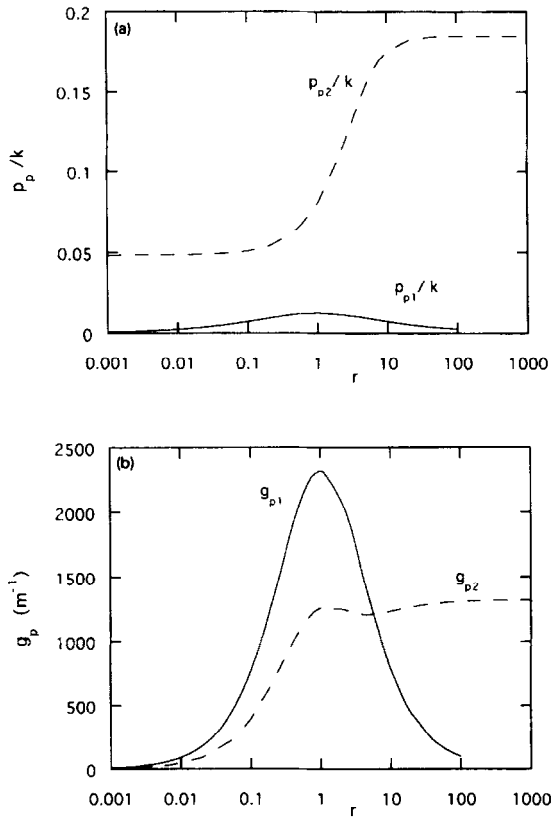


Fig. 3. Dependence of (a) the two global peak spatial-frequencies and (b) of their respective gains on $r$ when $E_0 = 5 \times 10^5$ V/m.

As we will see in the next section, in the low spatial-frequency domain, the behavior of the MI gain curve $g_{g1}$ (given by Eq. (13)) is approximately identical to that obtained from a local treatment of the space-charge field. This local gain is depicted in Fig. 1 by the long-dashed line curve. On the other hand, in the high spatial-frequency region, the MI gain approximately coincides with the gain arising from two-wave-mixing (TWM) [12], shown in Fig. 1 by a short-dashed line. Note that this latter process is antisymmetric with respect to the spatial-frequency (or $p/k$) and is known to cause fanning of broad optical beams [17]. Therefore, if for a given set of $E_0$ and $r$, $g_{p2}$ exceeds $g_{p1}$, one should then anticipate that the TWM fanning process will dominate the picture and will in turn strongly compete with modulational instability. Hence, from this point on, the gain associated with peak 1 will be the one that we will be referring to as the MI peak. Moreover, the dependence of $p_{p1}$ on $E_0$ and $r$, allows one to externally control the spatial period of the spontaneously generated filaments.

Finally, let us provide an example by considering the same parameters used to obtain Fig. 1. In this case, the MI peak gain and spatial-frequency are found to be $g_{p1} = 2.3 \times 10^3$ $m^{-1}$ and $p_{p1} = 3.7 \times 10^5$ $m^{-1}$, respectively. These results indicate that, in a 1 cm long SBN crystal, spatial noise at $p/k = 1.26 \times 10^{-2}$, or 0.72°, will experience $e^{23.3} \approx 10^{10}$ amplification. Such noise can always originate from scattering as well as from striations within the PR crystal. For this example, the spatial period of the spontaneously generated filaments is expected to be approximately 17 μm.

## 4. Modulational instability in the absence of higher-order effects

In this section we will also provide for completeness a local treatment of the MI process by neglecting higher-order effects in the space-charge field equation. A similar approach was followed in previous investigations of steady-state PR solitons where it was assumed that the drift nonlinearity dominates the PR process [3,4]. In particular, by assuming that the bias field is strong enough and that the optical beam is relatively broad, all the terms associated with the process of diffusion ($K_B T$ terms) can be ignored in Eq. (2). Moreover, under these conditions, the dimensionless term $\{[\epsilon_0 \epsilon_r/(eN_A)](\partial E_{sc}/\partial x)\}$ is typically much less than unity. From the above, the space-charge field is locally given by

$$E_{sc} = \frac{E_0}{1 + |U|^2}, \tag{14}$$

in which case the evolution equation, Eq. (1), takes the form [4]

$$i\frac{\partial U}{\partial z} + \frac{1}{2k}\frac{\partial^2 U}{\partial x^2} - \beta E_0 \frac{U}{1 + |U|^2} = 0. \tag{15}$$

Eq. (15) has the form of a nonlinear Schrödinger equation with a saturable nonlinearity and is known to allow solitary wave solutions [4]. Moreover, the spatial width and shape of these self-trapped states

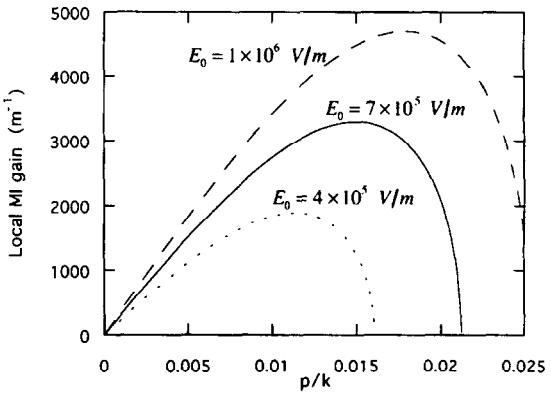


Fig. 4. Local MI gain as a function of $p/k$ for $E_0 = 4\times10^5$ V/m, (short-dashed line) $E_0 = 7\times10^5$ V/m (solid line), and $E_0 = 1\times10^6$ V/m (long-dashed-line) when $r = 1$.

were also found to depend only on two parameters, namely $E_0$ and $r$.

The MI properties of Eq. (15) can then be investigated by substituting Eq. (4) in Eq. (15) and by linearizing in $\epsilon$, i.e. through the evolution equation:

$$i\frac{\partial\epsilon}{\partial z} + \frac{1}{2k}\frac{\partial^2\epsilon}{\partial x^2} + \beta E_0 \frac{r}{(1+r)^2}(\epsilon + \epsilon^*) = 0. \tag{16}$$

Using a procedure similar to that of Ref. [18], the local MI gain associated with Eq. (16) can be readily obtained and is given by

$$g_{lc} = \mathrm{Re}\left\{\left(\frac{p^2}{k}\beta E_0 \frac{r}{(1+r)^2} - \frac{p^4}{4k^2}\right)^{1/2}\right\}. \tag{17}$$

Eq. (17) clearly indicates that the local MI gain, $g_{lc}$, is possible only for positive values of $E_0$ and, thus, its behavior is approximately the same as that of peak 1 of the global MI gain. The local MI gain is plotted in Fig. 1 (long-dashed line) for the same system parameters used to obtain the global MI gain. Note that Eq. (17) could have been directly obtained from Eq. (13) by setting $\Delta = \gamma = T = 0$, in which case $G(p) = \beta E_0 r/(1+r)^2$. A result similar to Eq. (17) was very recently obtained by Castillo et al. [10].

Fig. 4 shows the MI local gain $g_{lc}$ as a function of the dimensionless ratio $p/k$ for three different values of $E_0$ when $r = 1$ and for the same system parameters previously considered. Obviously, the maximum local MI gain as well as the corresponding spatial-frequency increase with $E_0$. Moreover, from Eq. (17) the maximum local MI gain and its associated spatial-frequency can be obtained and they are given by

$$g_{max} = \frac{k_0 n_e^3 r_{33} E_0}{2}\frac{r}{(1+r)^2}, \tag{18}$$

and

$$p_{max} = k_0 n_e^2 (r_{33} E_0)^{1/2}\frac{r^{1/2}}{(1+r)}. \tag{19}$$

A close examination of Eqs. (18) and (19) reveals that both $g_{max}$ and $p_{max}$ attain a maximum when $r = 1$ and, moreover, that they increase with $E_0$. Once again, this behavior is similar to that of the global MI peak previously obtained.

To further study the MI process (under local conditions), Eq. (15) was solved numerically using a beam propagation method [15,19]. A very broad bright-like optical beam [20] was used as the input beam profile. Numerical errors, inherent to the numerical procedure, provided the noise source. Fig. 5 depicts the evolution of the beam intensity profile when $E_0 = 4\times10^5$ V/m, $r = 1$ and for the same system parameters previously considered. This figure also shows that the spatial filaments first develop on the top of the input optical beam, where the intensity ratio is approximately 1. Fig. 6, on the other hand,

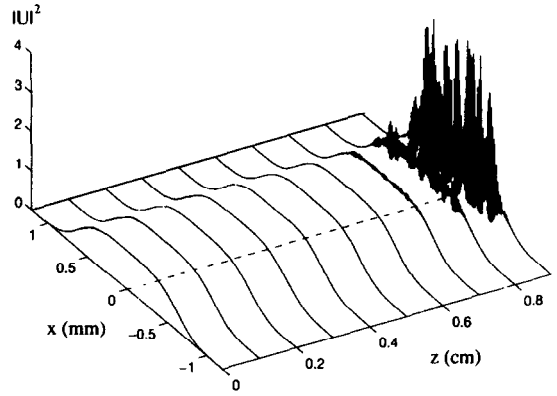


Fig. 5. Intensity profile evolution of a broad optical beam when $E_0 = 4\times10^5$ V/m and $r = 1$.

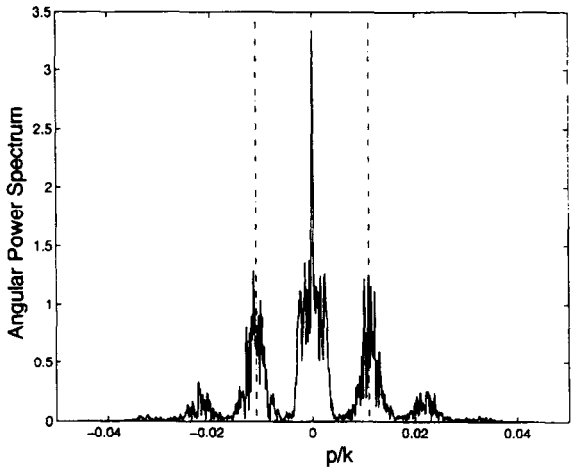


Fig. 6. Angular power spectrum of a broad optical beam at $z = 0.9$ cm (solid line) and $p_{max}/k$ predicted from theory (dashed line) when $E_0 = 4 \times 10^5$ V/m and $r = 1$.

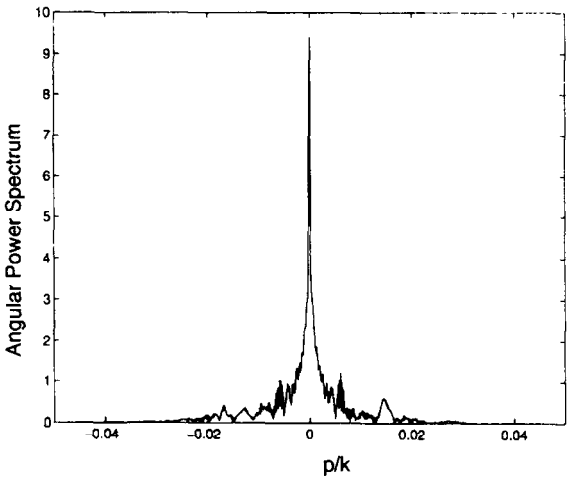


Fig. 8. Angular power spectrum of a broad optical beam at $z = 1$ cm when $E_0 = 4 \times 10^5$ V/m and $r = 4$.

illustrates the angular power spectrum of the same optical beam (solid line curve) at $z = 0.9$ cm under the same conditions. Moreover, in Fig. 6 we have also plotted (dashed line) the value of $p_{max}/k$ obtained from Eq. (19), which in this case is 0.011. Evidently, the two results are in good agreement. Fig. 7 shows the evolution of the optical beam intensity when $r = 4$, $E_0 = 4 \times 10^5$ V/m, and for the same system parameters. A close inspection of this figure reveals that the spatial filaments now develop on the sides of the optical beam where the normalized intensity is approximately equal to unity.

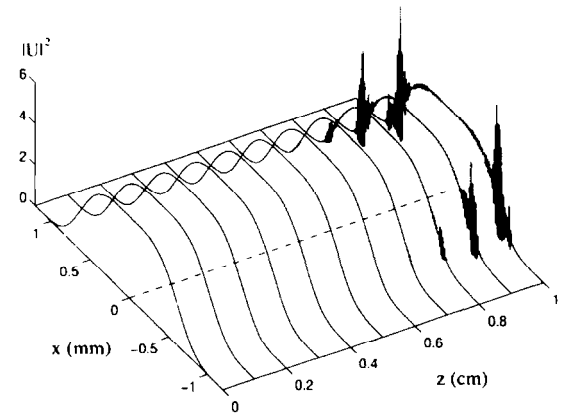


Fig. 7. Intensity profile evolution of a broad optical beam when $E_0 = 4 \times 10^5$ V/m and $r = 4$.

This should have been anticipated, since $g_{max}$ attains a maximum at $r = 1$. However, the results of our theory can only be taken approximately in this case, since the optical envelope is no longer constant on the sides of the optical beam. Moreover, for the same reason, one should expect a richer angular spectrum than the one of Fig. 6. Fig. 8 shows the angular power spectrum at $z = 1$ cm for the same conditions used in obtaining Fig. 7. Note that, in this case, the angular power spectrum is somewhat more involved, since the MI first appears on the sides of the optical beam.

## 5. Conclusions

In conclusion, we have investigated the modulational instability of broad (quasi-plane-wave) optical beams in biased PR media under steady-state conditions. The spatial growth rate of the sideband perturbations was obtained by globally treating the space-charge field equation. Our analysis indicates that the MI growth rate depends on the strength and polarity of the external bias electric field and, moreover, on the ratio of the optical beam intensity to that of the dark irradiance. This, of course, may allow one to externally control the spatial period of the spontaneously generated filaments. Our results were then compared to previous procedures where the MI gain

was considered by locally treating the space-charge field. The two approaches were found to be in good agreement in the low spatial-frequency regime provided that the external bias field is relatively strong. In this region, we have found that the instability growth rate increases with the bias field and that it attains a maximum when the optical beam intensity is approximately equal to the dark irradiance. Conversely, in the high spatial-frequency regime, notable differences may exist between these two treatments. In particular, our results show that, under low bias conditions, beam fanning originating from two-wave-mixing may dominate the picture and will thus strongly compete with modulational instability. In this regime, further experimental studies may be required so as to better understand the competition of these two processes (MI and TWM) in the evolution of the angular power spectrum.

## Acknowledgements

The authors would like to thank M. Segev for useful discussions. This work was supported in part by JNICT of Portugal. M.I. Carvalho is also with Centro de Optoelectronica, INESC, R. Jose Falcão 110, 4000 Porto, Portugal.

## References

[1] M. Shih, M. Segev, G.C. Valley, G. Salamo, B. Crosignani, and P.D. Porto, Electron. Lett. 31 (1995) 826.

[2] M.D. Castillo, A. Aguilar, J.J. Mondragon, S. Stepanov, and V. Vysloukh, Appl. Phys. Lett. 64 (1994) 408.

[3] M. Segev, G.C. Valley, B. Crosignani, P.D. Porto, and A. Yariv, Phys. Rev. Lett. 73 (1994) 3211.

[4] D.N. Christodoulides and M.I. Carvalho, J. Opt. Soc. Am B 12 (1995) 1628.

[5] M. Segev, B. Crosignani, A. Yariv, and B. Fischer, Phys. Rev. Lett. 68 (1992) 923.

[6] B. Crosignani, M. Segev, D. Engin, P.D. Porto, A. Yariv, and G. Salamo, J. Opt. Soc. Am. B 10 (1993) 446.

[7] D.N. Christodoulides and M.I. Carvalho, Opt. Lett. 19 (1994) 1714.

[8] V.I. Bespalov and V.I. Talanov, JETP Lett. 3 (1966) 307.

[9] K. Tai, A. Tomita, J.L. Jewell, and A. Hasegawa, Appl. Phys. Lett. 49 (1986) 236.

[10] M. Iturbe-Castillo, M. Torres-Cisneros, J. Sanchez-Mondragon, S. Chavez-Cerda, S. Stepanov, V. Vysloukh, and G. Torres-Cisneras, Opt. Lett. 20 (1995) 1853.

[11] V.E. Zakharov and A.M. Rubenchik, Sov. Phys. JETP 38 (1974) 494.

[12] P. Gunter and J.P. Huignard, eds., Photorefractive Materials and Their Applications I and II (Springer-Verlag, Berlin, 1988);
P. Yeh, Photorefractive Nonlinear Optics (Wiley, New York, 1993).

[13] Note that the dark irradiance $I_d$ can be elevated artificially, as done in Ref. [2].

[14] N. Kukhtarev, V.B. Markov, S.G. Odulov, M.S. Soskin, and V.L. Vinetskii, Ferroelectrics 22 (1979) 949;
V.L. Vinetskii and N.V. Kukhtarev, Sov. Phys. Solid State 16 (1975) 2414.

[15] G.P. Agrawal, Nonlinear Fiber Optics (Academic Press, Boston, Mass., 1989).

[16] R.A. Vazquez, R.R. Neurgaonkar, and M.D. Ewbank, J. Opt. Soc. Am. B 9 (1992) 1416.

[17] M. Segev, Y. Ophir, and B. Fischer, Opt. Comm. 77 (1990) 265.

[18] A. Hasegawa and W.F. Brinkman, IEEE J. Quantum electron. QE-16 (1980) 694.

[19] S.R. Singh and D.N. Christodoulides, Opt. Comm. 118 (1995) 569.

[20] A super-Gaussian was used as the input beam: $U = r^{1/2} \exp[-(x/b)^4]$, where $b = 800$ μm.